ИНФОРМАЦИЯ О СТАТЬЕ НА РУССКОМ ЯЗЫКЕ

DOI:10.18503/1995-2732-2016-14-1-79-87

ОБРАЗОВАНИЕ ГОРЯЧИХ ТРЕЩИН В НИЗКОЛЕГИРОВАННОЙ СТАЛИ: ИССЛЕДОВАНИЕ КРИТИЧЕСКИХ РЕЖИМОВ

Брунелли К., Бруски С., Джотти А., Ленчина Р., Дабала М.

Департамент индустриальной инженерии Университета г. Падуя, Италия

Аннотация. В работе изучено влияние температуры на рост хрупких трещин и, соответственно, на изменение механических свойств стали марки 20Mn4. На термомеханической моделирующей установке Gleeble 3800™ проведены испытания на одноосное растяжение в диапазоне температур от 1000 до 1280°С. Термические обработки при разных температурах и времени выдержки осуществлялись в трубчатой печи.

После проведенных испытаний на растяжение и термических обработок образцы были проанализированы при помощи растровой электронной микроскопии для оценки влияния эволюции микроструктуры на протекание горячеломкости. Явление горячеломкости в основном обусловливает скопление меди на поверхности раздела металл-окалина: в характерном диапазоне температуры жидкая фаза, обогащенная медью, проникает по всем границам зерен, способствуя образованию трещин и проявлению горячеломкости.

Ключевые слова: сталь, термическая обработка, горячеломкость, механические свойства, эволюция микроструктуры.

Hot shortness cracks formation in a low alloy steel: investigation on the critical conditions / Brunelli K., Bruschi S., Ghiotti A., Lencina R., Dabalà M. // Вестник Магнитогорского государственного технического университета им. Г.И. Носова. 2016. Т. 14. №1. С. 79–87. doi:10.18503/1995-2732-2016-14-1-79-87

Brunelli K., Bruschi S., Ghiotti A., Lencina R., Dabalà M. Hot shortness cracks formation in a low alloy steel: investigation on the critical conditions. *Vestnik Magnitogorskogo Gosudarstvennogo Tekhnicheskogo Universiteta im. G.I. Nosova* [Vestnik of Nosov Magnitogorsk State Technical University]. 2016, vol. 14, no. 1, pp. 79–87. doi:10.18503/1995-2732-2016-14-1-79-87

UDC 620.2

DOI:10.18503/1995-2732-2016-14-1-87-100

BAINITE STEEL: STRUCTURE AND WORK HARDENING

Gromov V.E.[1], Nikitina E.N.[1], IvanovYu.F.[2,3], Aksenova K.V.[1], Semina O.A.[1]

[1] Siberian State Industrial University, Novokuznetsk, Russia
[2] Institute of high–current electronics SB RAS, Tomsk, Russia
[3] National Research Tomsk Polytechnic University, Tomsk, Russia

Abstract. Using the methods of transmission electron diffraction microscopy, a quantitative evolution analysis of defective and carbide subsystems of medium-carbon steel with a bainite structure under a compression strain up to 36% has been performed. A quantitative analysis of carbon redistribution has been carried out, as well as the dependence established of the concentration of carbon atoms arranged in a crystal lattice of α- and γ-iron on structural defects in cementite particles lying in a number of bainite plates and intra-phase boundaries, and on the degree of deformation.

It has been demonstrated that scalar dislocation density, material volume with deformation twins, a number of stress concentrators, the amplitude of crystal lattice curvature-torsion, the disorientation degree of fragments are increased with the growth of the degree of deformation and average longitudinal fragment sizes are decreased. The long-range stress fields have been estimated. The possible causes of the different stages of parameter changes of the carbide phase and dislocation substructure with deformation have been discussed.

Strengthening mechanisms with the boundaries of the plates and fragments, scalar dislocation density, long-range stress fields, and cementite particles, the interstitial atoms have been estimated. It has been shown that the largest contribution to the amount of work hardening of the steel examined leads to substructural hardening (hardening due to long-range internal stress fields and structure fragmentation) and solid-solution hardening, due to the introduction of carbon atoms into the crystal lattice of the ferrite.

It has been suggested that the cause of softening of steel with a bainite structure at high (over 15%) degrees of deformation is the activation of the process of deformation fine-scale twinning.

Keywords: hardening, bainite, deformation, cementite, dislocation substructure, mechanisms, steel.

1. Introduction

Recently the attention of researches in the field of physical metallurgy is paid to the study of features of bainite transformation in steels [1–5]. Steels with bainite structure are widely used in manufacture of large diameter pipes, power engineering, automobile industry, production of rails, etc. [6–10].

Bainite steels, by virtue of transformation $\gamma \rightarrow \alpha$ features, have a complex multiphase structure being formed as a result of superposition of shear and diffusion mechanisms of transformation [11, 12]. The main factors determining properties of bainite structure steel can include: the availability of carbon atoms and other alloying elements in iron crystal lattice; boundaries of grains, packets, crystals of bainite; cementite particles; inclusions of retained austenite; dislocations and internal stress fields caused by structural elements [13–16]. A knowledge of quantitative regularities and mechanisms of work hardening of steel with bainite structure allows to control purposefully the structure-phase states of steel and its mechanical properties [11, 17, 18].

For revealing the promising fields of technologies' application based on plastic deformation following heat treatment it is necessary to study the dependence of hardening effect on structural state of the material and deformation treatment parameters, to establish cause and effect relationships between the phenomena determining the complex improvement of properties [19]. In its turn, a knowledge of regularities of structure formation and steel properties in plastic deformation is necessary for control the process of work hardening.

The characteristics of carbide phase and dislocation substructure are not determined by methods of optical and scanning electron microscopy and can reliably be revealed with application of transmission electron microscopy [11, 20, 21]. Apparent scientific and practical importance of such results is determined by the fact that the understanding of physical nature and basic parameters of formation and evolution of structure-phase states and dislocation substructure is a necessary condition for development of physical material science of bainite steels.

The aim of the research was to investigate the evolution of carbide subsystem, defective substructure, distribution of carbon atoms in structural steel with bainite structure under compression plastic deformation and to reveal the mechanisms of its work hardening.

2. Materials and Methods

Structural steel 30Cr2Ni2MoV was used as a test material [22]. Austenization of steel was done at temperature 960°C during a period of 1.5 hours; cooling was done in air. Deformation of steel was carried out by uniaxial compression of columns 4×4×6 mm^3 in size at a rate $\sim 7 \cdot 10^{-3}$ s^{-1} on testing machine "Instron-1185". Compression as a method of deformation was convenient to use because, in this case, it was possible to reach the deeper deformations than in extension. Investigations of steel structure and phase composition were performed by methods of electron diffraction microscopy of thin foils [11, 19].

3. Results and Discussion

A characteristic form of curves of steel work hardening is shown in Fig 1, **a**. Mathematical treatment of curves of work hardening shows that σ–ε relation has a periodic form and is described by polynomial of the fourth power. Differentiation of σ–ε relation curve makes possible to determine the coefficient of steel work hardening $\theta = \frac{\partial \sigma}{\partial \varepsilon}$.

When analyzing the results shown in Fig. 1, b, two stages of work hardening can be singled out: a stage with parabolic σ–ε relation or decreasing coefficient of hardening Θ and a stage with a slightly changing negative value of coefficient of hardening. Transition from the first stage to the second one occurs in the interval of deformation degree (19…25) %. Failure of steel samples being tested took place at $\varepsilon \approx 0.4$ by brittle cleavage with the formation of some coarse fragments. It is apparent that deformation behavior of samples is conditioned by the change of phase composition and defective substructure of the material.

As a result of bainite transformation on continuous cooling of steel a multiphase structure is formed which is presented by α-phase (solid solution based on *bcc* (body-centered cubic) crystal lattice); γ-phase (solid solution based on *fcc* (face-centered cubic) crystal lattice) and iron carbide (in low- and medium-carbon steels – cementite). The characteristic image of bainite structure of steel 30Cr2Ni2MoV is presented in Fig 2.

Deformation of steel is accompanied by changing the state of carbide phase. The increase in degree of deformation results in reduction of average sizes (Fig. 3), density and volume fraction (Fig. 4) of iron carbide particles. At the same time the morphology of particles changes. First, their spatial form transforms: initially lamellar particles (ratio of longitudinal sizes (L) to transverse ones (d) $L / d \approx 8$) transform into ellipsoidal ones ($L / d = \approx 5$) (Fig. 3, insertion) at the last stage of deformation.

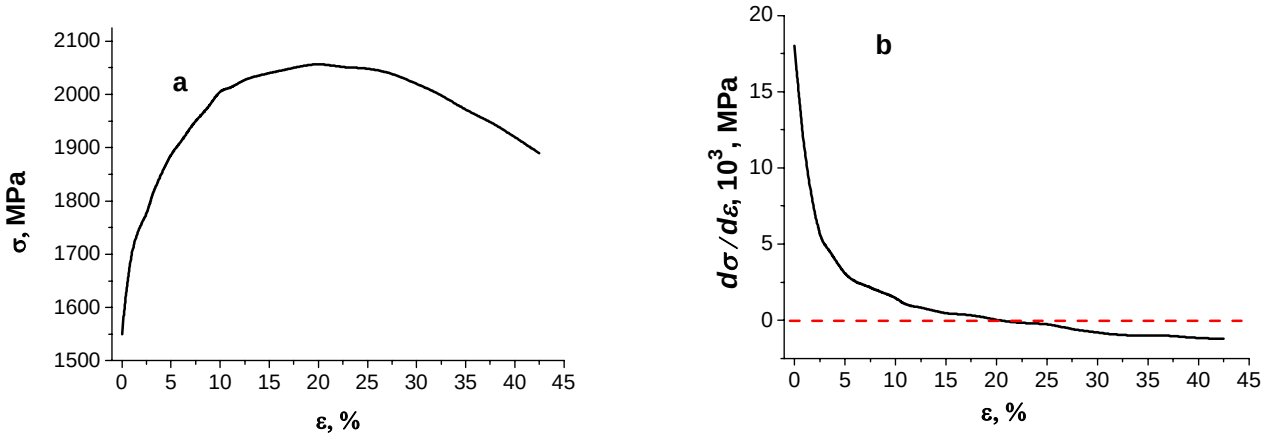

Fig. 1. Strain hardening curve (**a**) and the dependence of strain hardening coefficient on deformation degree (b) of steel with bainite structure

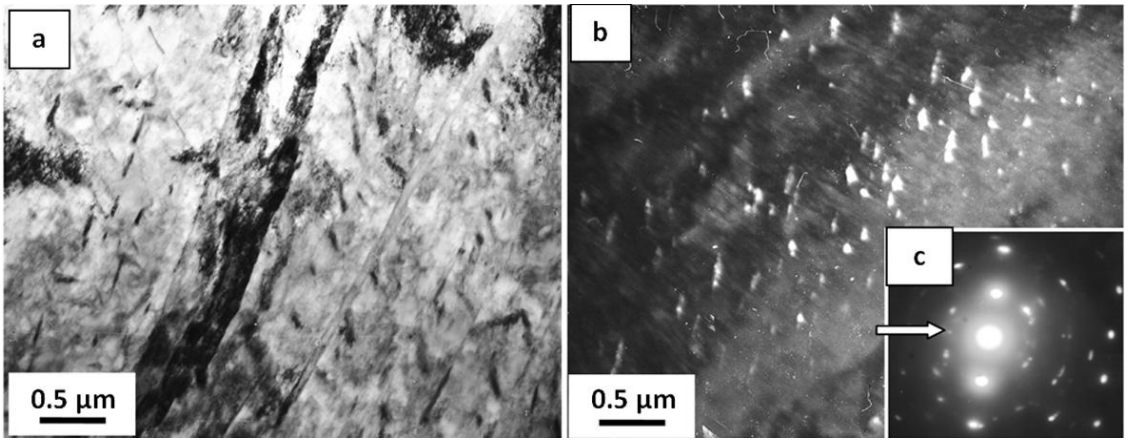

Fig. 2. Electron microscope image of the structure of 30Cr2Ni2MoV steel, formed as a result of cooling from the temperature of austenization; **a** – light field image; b – dark field, received in reflection [201]Fe_3C; c – microelectron diffraction pattern, the arrow indicates the reflection, in which the dark field is received

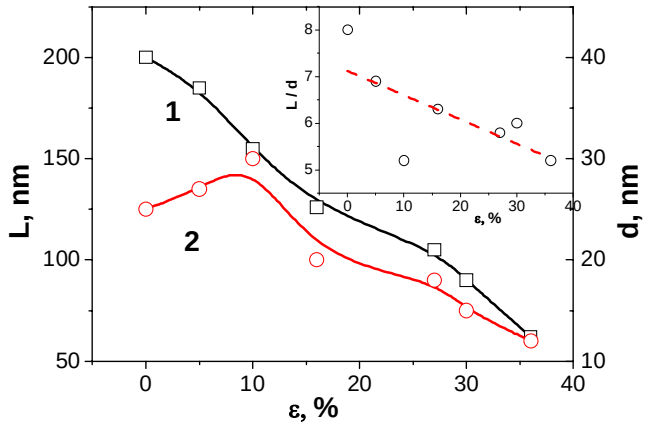

Fig. 3. Dependence of longitudinal L (curve 1) and transverse d (curve 2) dimensions of cementite particles, located in the volume of bainite crystals on deformation degree of steel **ε**

Second, place of location of cementite particles changes: with the increase in degree of deformation the volume fraction of particles located on the boundaries of bainite plates increases markedly (Fig. 4, curve 1).

The behavior of total volume fraction of cementite (Fig. 4, curve 3) is noteworthy. The initial stage of deformation ($\varepsilon \approx 10\%$) is accompanied by the increase in total fraction of cementite particles in steel; at large degrees of deformation the volume fraction of cementite in steel decreases. It is clear that the increase in total fraction of cementite particles under small degrees of deformation is connected with transformation of retained austenite with formation of cementite initiated by deformation of steel. In fact, the carried out electron microscopy diffraction patterns have revealed the fact of rapid decrease in volume fraction of retained austenite already at low ($\varepsilon \approx 10\%$) degrees of steel deformation (Fig. 4, b).

Third, inside of bainite crystals (on dislocations and boundaries of fragments) the particles of round shapes whose quantity increases with the growth of deformation degree are detected (Fig. 5).

The discovered quantitative regularities of changing the parameters of steel structure in the process of plastic deformation enabled the investigations directed to the analysis of carbon atom distribution in the structure of the deformed steel to be carried out.

Estimates of relative content of carbon atoms on structural elements of steel were carried out using the expressions generalized in Table. 1. The results of the carried out estimates are given in Fig. 6.

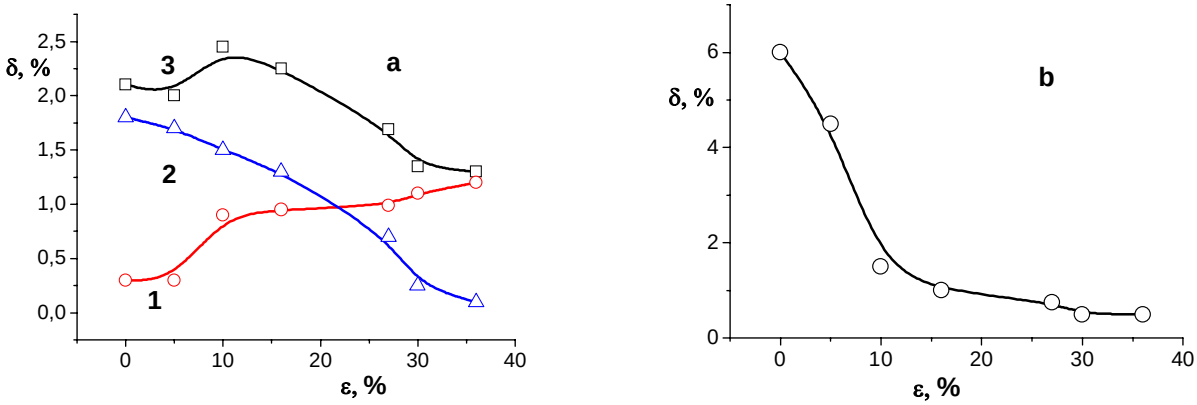

Fig. 4. Dependence of volume fraction of cementite particles (**a**) and retained austenite layers (b) on deformation degree of steel **ε**; curve 1 – cementite particles, located on the boundaries of ferrite crystals, curve 2 – in ferrite crystals; curve 3 demonstrates the changes of the total volume fraction of cementite in steel

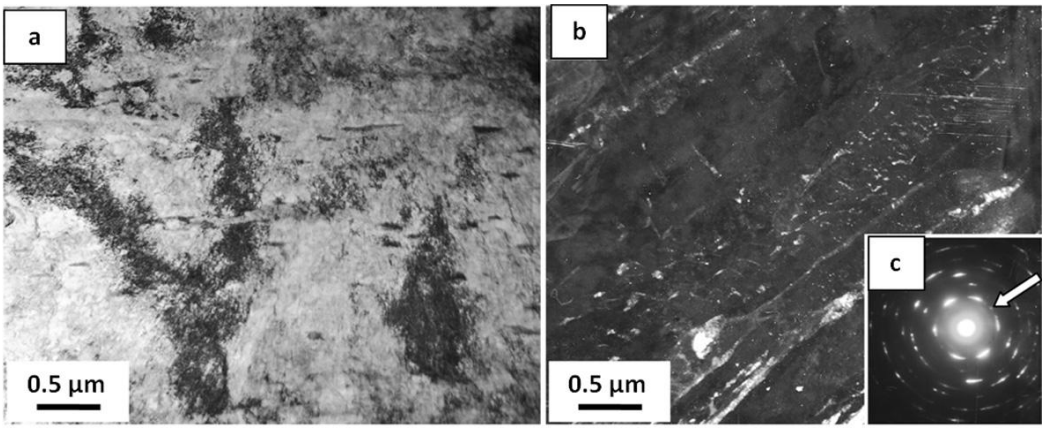

Fig. 5. Electron microscope image of 30Cr2Ni2MoV steel structure, subjected to an uniaxial compression at **ε** ≈ 36%; **a** – light field image; b – dark field, received in reflection [211]Fe_3C; **c** – microelectron diffraction pattern, the arrow indicates the reflection, in which the dark field is received

Table 1

Method of analysis of carbon distribution in steel

Regions of carbon locations	Estimate expression
Solid solution based on α-iron	$\Delta C_\alpha = \Delta V_\alpha \frac{a_\alpha - a_\alpha^0}{39 \pm 4} \cdot 10^3$ *
Solid solution based on γ-iron	$\Delta C_\gamma = \Delta V_\gamma \frac{a_\gamma - a_\gamma^0}{44} \cdot 10^3$
Particles of carbide phases	$\Delta C_к = \Delta V_k \cdot k$; $k(Fe_3C) = 0{,}07$
Elements of defective structure	$\Delta C_д = C_0 - (\Delta C_\alpha + \Delta C_\gamma + \Delta C_к)$

*Here ΔV_α, ΔV_γ, ΔV_k – volume fraction α-γ-Fe and carbide phases, respectively; a_α, a_γ – present parameter of lattice of α- and γ-phase, respectively; $a_\alpha^0 = 0{,}28668nm$, $a_\gamma^0 = 0{,}3555nm$; C_0 – average content of carbon in steel.

The carried out estimates showed that with the increase in degree of deformation the quantity of carbon atoms located in solid solution based on α-iron (Fig. 6, curve 1), in cementite particles lying on intraphase boundaries (Fig. 6, curve 2), and those located on defects of crystal structure (Fig. 6, curve 3), increased. The quantity of carbon atoms forming cementite particles lying in the volume of bainite plates (Fig. 6, curve 4), and located in solid solution based on γ-iron (Fig. 6, curve 5), is reduced. Thus, plastic deformation of steel with bainite structure is accompanied by appreciable redistribution of carbon atoms. If in the initial state the basic quantity of carbon atoms was concentrated in cementite particles, then at the final stage of deformation the preferable location of carbon is crystal lattice based on α-iron.

Martensite (shear) mechanism of ferrite formation leads to the formation of dislocation substructure of net-like type with a relatively high scalar density of dislocations measuring $\approx 7 \times 10^{10}$ cm^{-2} in the tested steel in bainite plates. Plastic deformation of steel leads to the increase in scalar density of dislocations (Fig. 7, **a**). In this case the type of dislocation structure is unchangeable – a net-like substructure is retained.

When analyzing the results shown in Fig. 7, **a**, two sections on the curve dependence of scalar density of dislocations on degree of deformation can be distinguished. On the first section (0% <ε< 18%) a linear increase in scalar density of dislocations is observed; on the second section (18% <ε< 36%) being equal to the first one in length the growth of density of dislocations is practically not revealed. This circumstance may be caused by both the difficulty of dislocation substructure analysis at densities of dislocations being larger than$\approx 10^{11}$ cm^{-2}, which is due to the overlapping of nuclei of closely-spaced dislocations and the possibility of realization of non-dislocation mechanism of material's deformation.

One of these mechanisms being realized under deformation can be twinning. In fact, the investigations carried out in the research detected the significant increase in volume of the material containing deformation microtwins under degree of deformation exceeding ≈18% (Fig. 7, b). The characteristic image of steel volume with microtwins of deformation origin is shown in Fig. 8.

Elastic stresses taking place in realization of shear mechanism of transformation γ→α result in not only the formation of substructure with a high scalar density of dislocations but fragmentation of bainite plates as well that is the partition of plates into regions with a low-angular disorientation that are most clearly defined by methods of dark field analysis.

Deformation of steel results in the decrease in average longitudinal sizes of fragments (transverse sizes of fragments are limited by the boundaries of bainite plates and are practically unchangeable under deformation) (Fig. 9, **a**). In this case, several stages are revealed in changing of sizes of fragments: at the first stage this process runs very intensively, at the second stage – significantly slower.

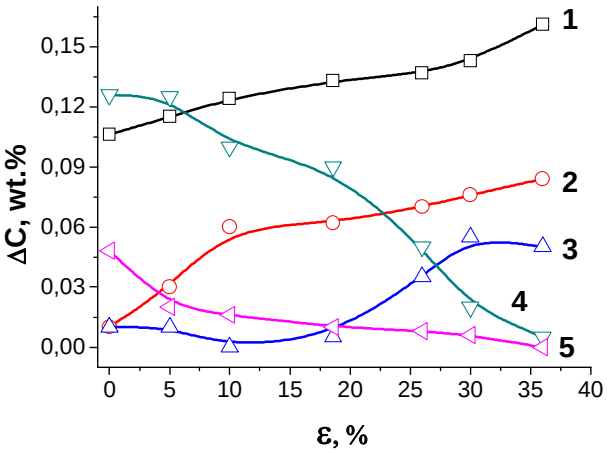

Fig. 6. Dependence of carbon atom concentration, located in a crystal lattice based on **α**-Fe (1), in cementite particles, lying on the internal phase boundaries (2), on structural defects (3), in cementite particles, lying in the volume of bainite plates (4), a crystal lattice based on **γ**-Fe (5) on deformation degree

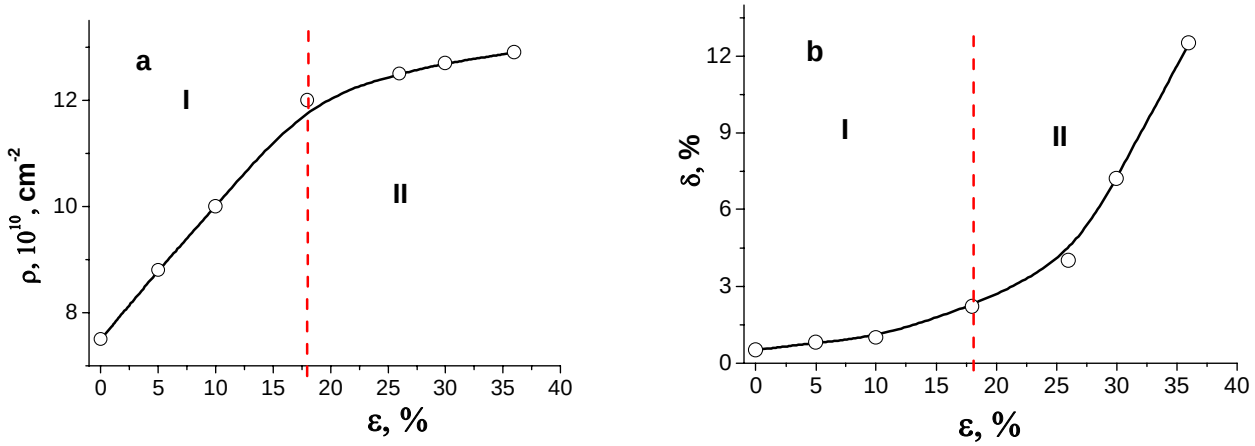

Fig. 7. Dependence of scalar density of dislocations (**a**) and material volume, containing microtwins (b) on deformation degree

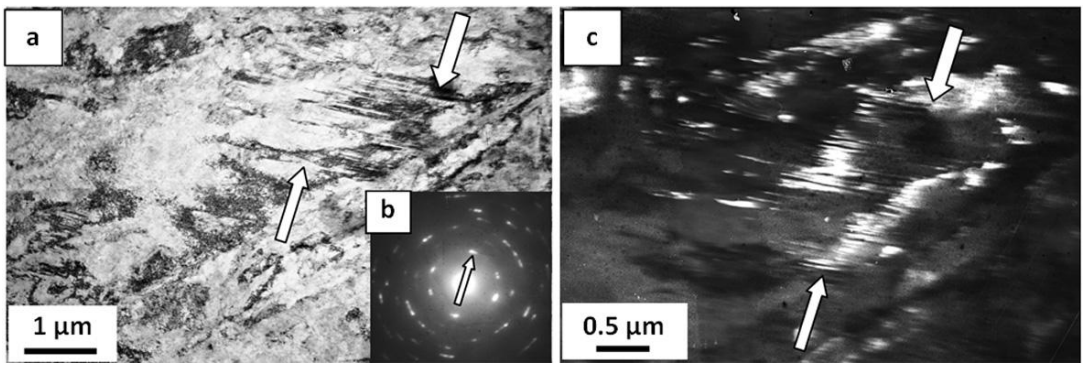

Fig. 8. Electron microscope image of steel structure following deformation **ε** = 36%; **a** – light field image; b – microelectron diffraction pattern; c – dark field, received in reflection [101]**α**-Fe; the arrows indicate: on (**a**) and (c) – microtwins of deformation origin; on (b) – reflection, in which the dark field is received

The changing of sizes of fragments goes on the backround of increase in degree of their disorientation (Fig. 9, b). Azimuthal constituent of the complete angle of disorientation was determined by the relative value of broadening of reflections of α-phase in accordance with the technique presented in [20]. When analyzing the results shown in Fig. 9, b, three stages of development of the process can be distinguished: at stages I and III the disorientation of substructure elements increases relatively slow, at stage II – it does significantly more intensive.

Deformation of steel is accompanied by the formation of internal fields of stresses that are revealed in analyzing the bend extinction contours by methods of electron microscopy of thin foils [19, 21, 23, 24].

The performed investigations showed that with the increase in degree of deformation the surface density of contours (Fig. 10, **a**) (a quantity of contours per unit area of the photograph) enhanced and their average transverse sizes decreased (Fig. 10, b). The first fact is indicative of the increase in number of stress concentrators in the material with rise of degree of deformation, the second one – the rise of amplitude of curvature-torsion of crystal lattice of the material and internal long-range fields of stresses, respectively [19, 21, 23, 24]. Simultaneously with it the shape of contours and their arrangement in bainite plates changes. If in the initial state and at low degrees of deformation the contours arranged predominantly transverse to the plates, crossing the plate from one boundary to the other, then following the large degrees of deformation (18% and more) ring contours encompassing some regions in the volume of plates are formed in the material.

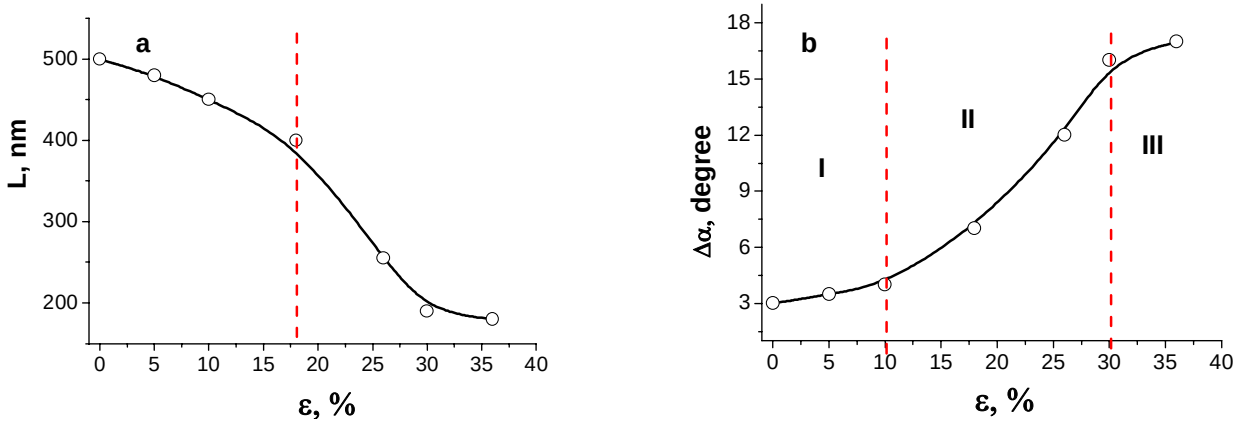

Fig. 9. Dependence of middle longitudinal dimensions of the fragments (**a**) and the value of an azimuthal component of a complete angle of substructure disorientation (b) on deformation degree

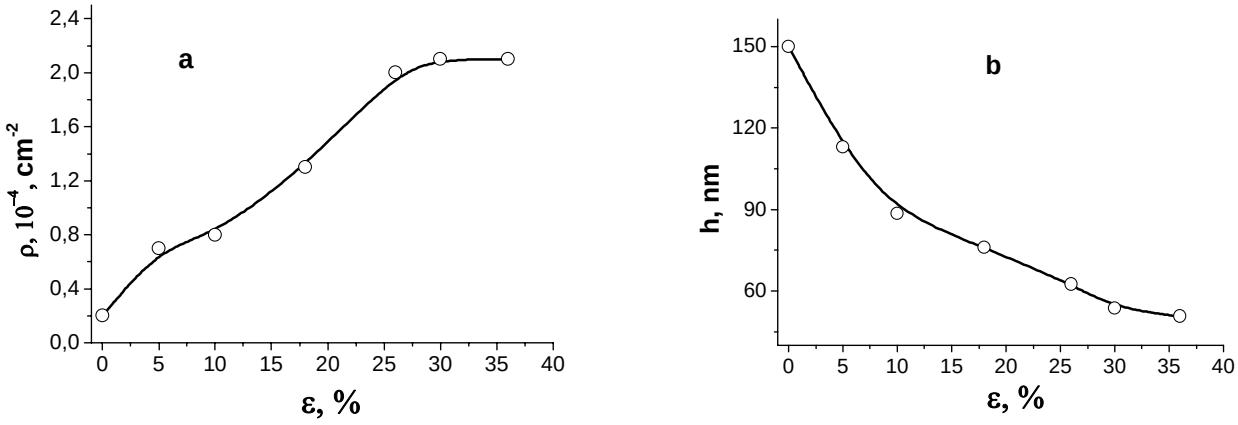

Fig. 10. Dependence of surface contour density (**a**)
and the middle transverse dimensions (b) on deformation degree

The regulations of parameter evolution of structure-phase states and defective substructure of steel under deformation detected above make it possible to analyze the mechanisms of work hardening.

Hardening of the material with low angular boundaries (substructural hardening, hardening with boundaries of plates and fragments) can be estimated using the expression [25]:

$$\sigma(L) = \sigma_0 + k^* L^{-m}, \quad (1)$$

where m = 1 or 1/2, L – effective size of ferrite plates and fragments being defined with effective length of slip plane in the plate. It is established that at m = 1 k varies from 0.015 to 0.01 kg/mm$^{3/2}$; at m = 1/2 k varies from 0.2 to 0.98 kg/mm$^{3/2}$ [25, 26].

Dependence of value of contribution from boundaries of fragments to work hardening of steel with bainite structure on degree of deformation is shown in Fig. 11, **a**. In calculations the following values of parameters included in the equation (1) were used: L – average longitudinal sizes of fragments; k = 0,015; m = 1. It is clearly seen that with increase in degree of deformation of steel the value of hardening by fragment boundaries increases within 330 to 790 MPa (Fig. 11, **a**), and it is caused by decrease in average sizes of fragments (Fig. 9, **a**).

The first term in the equation (1) σ_0 is friction stress of material's lattice that is stress necessary for motion of dislocations in pure monocrystals (for example, Peierls stress for pure metals). Consequently, stress σ_0 depends substantially on degree of material's purity and value of its work hardening. For theoretically pure material σ_0 = 17 MPa. The experimentally determined values σ_0 vary within 27 to 60 MPa [27, 28]. For steels value σ_0 = 30–40 MPa [29].

As noted above, a dislocation substructure of net-like type with a relatively high scalar density of dislocations measuring ≈7×10^{10} cm^{-2} is revealed in ferrite plates having been formed as a result of shear (martensite) mechanism of transformation. Plastic deformation of steel is accompanied by growth of scalar density of dislocations (Fig. 7, **a**). In this case the type of dislocation substructure is unchangeable.

Stress needed for supporting a plastic deformation i.e. flow stress σ is connected with density of dislocations in the following manner [27, 30, 31]:

$$\sigma = \sigma_0 + k\sqrt{\rho}, \quad (2)$$

where σ_0 – flow stress of non-dislocation origin (i.e. caused by other mechanisms of hardening); ρ – average (scalar) density of dislocations; $k = m\alpha Gb$; m – Schmidt orientation factor; α – parameter characterizing the value of interdislocation interaction being equal 0.1...0.51 [28, 32]; G – shear modules (≈80 GPa); b – Burgers vector of dislocation (0.25 nm). For steels with regard to orientation factor m, $m\alpha \approx 0.5$ is usually taken.

In Fig. 11, b the dependence of value of contribution, being determined by scalar density of dislocations, to the work hardening of steel under study on degree of deformation is shown. It is clearly seen that with the increase in degree of deformation of steel the value of the given contribution is increased proportionally to the growth of scalar density of dislocations varying within the limits of 280 MPa to 360 MPa.

The long-range fields of internal stresses play an important part in formation of yield point, work hardening and failure of crystalline materials. The application of method of electron diffraction microscopy enables one to analyze the value of internal stresses according to of material's structure by several methods: 1) according to radius of segment bending of free dislocations [33, 34]; 2) according to distance between dislocations and parameters of dislocation aggregates [35]; 3) according to distance between active slip planes [36]; 4) according to parameters of bend extinction contours [24]. The fourth method was used in studying the long-range internal fields of stresses in this research.

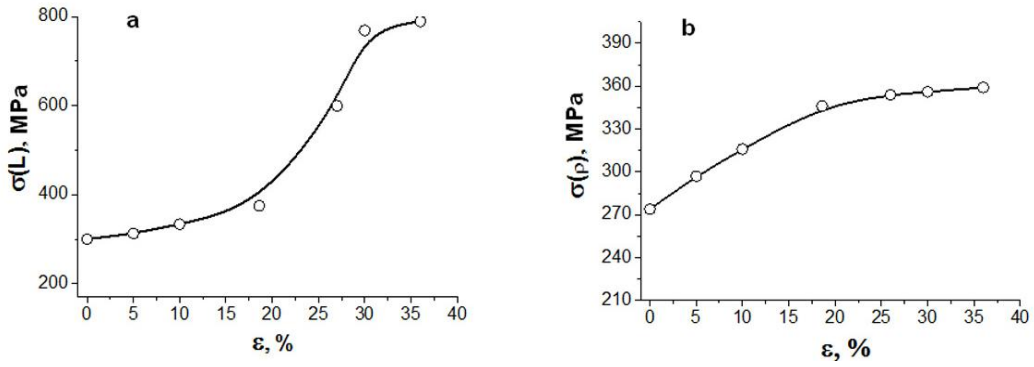

Fig. 11. Dependence of contribution into the flow stress from the boundaries of fragments (**a**) and dislocation «forest» (b) on deformation degree

The procedure of estimation of value of internal stress fields consists in determining the curvature-torsion gradient of crystal lattice χ [37]:

$$\chi = \frac{\partial \varphi}{\partial \ell} = \frac{0,017}{h}, \quad (3)$$

where h – transverse sizes of bend extinction contour.

Further, value of excessive density of dislocations $\rho_{\pm} = \rho_{+} + \rho_{-}$ (ρ_{+} and ρ_{-} – density of positively and negatively charged dislocations correspondingly) is estimated [21, 37]:

$$\rho_{\pm} = \frac{1}{b} \cdot \frac{\partial \varphi}{\partial \ell}. \quad (4)$$

Value of long-range fields of internal stresses is estimated on the basis of the relation [19]:

$$\sigma(h) = \alpha_C G b \sqrt{\rho_{\pm}} = \alpha_C G b \sqrt{\frac{1}{b} \cdot \frac{\partial \varphi}{\partial \ell}} = \\ = \alpha_C G \sqrt{\frac{0.017 \cdot b}{h}}, \quad (5)$$

where $\alpha_c = 1$ – Strunin coefficient [38], h – average transverse sizes of bend extinction contour.

Investigations carried out in this research showed that average transverse sizes of contours decreased with the growth of degree of deformation of steel (Fig. 10, b). Following the expression (5) value of long-range fields of internal stresses will increase (Fig. 12, a).

Bainite steel is characterized by the presence of cementite particles in the structure. The particles are obstacles to motion of dislocations and lead to hardening of the material. Owing to it yield point of the material σ_y increases by value $\Delta\sigma_P$

$$\sigma_y = \sigma_0 + \Delta\sigma_P \quad (6)$$

Estimates of steel hardening under deformation taking into account the presence of cementite particles should be carried out using relations obtained for in-coherent precipitations [39]:

$$\sigma_{op} = M \frac{mG_m b}{2\pi\left(|\lambda - D|\right)} \Phi \cdot \ln\left(\left|\frac{\lambda - D}{4b}\right|\right), \quad (7)$$

where λ – average distance between particles, D – average size of particles, m – orientation factor being equal to 2.75 [40] for *bcc* lattice of materials, Φ =1 for screw and $\Phi = (1-\nu)^{-1}$ for edge dislocations, M – parameter considering the nonuniformity of distribution of particles in matrix being equal to 0.81...0.85 [39].

In Fig. 12, b the relation of value of contribution to flow stress of cementite particles on degree of steel deformation with bainite structure is illustrated. It is clearly seen that the value of the contribution varies in a complex way within ranges 210 to 260 MPa. It can be caused by process of dissolution and repeat precipitation of cementite particles under deformation of steel.

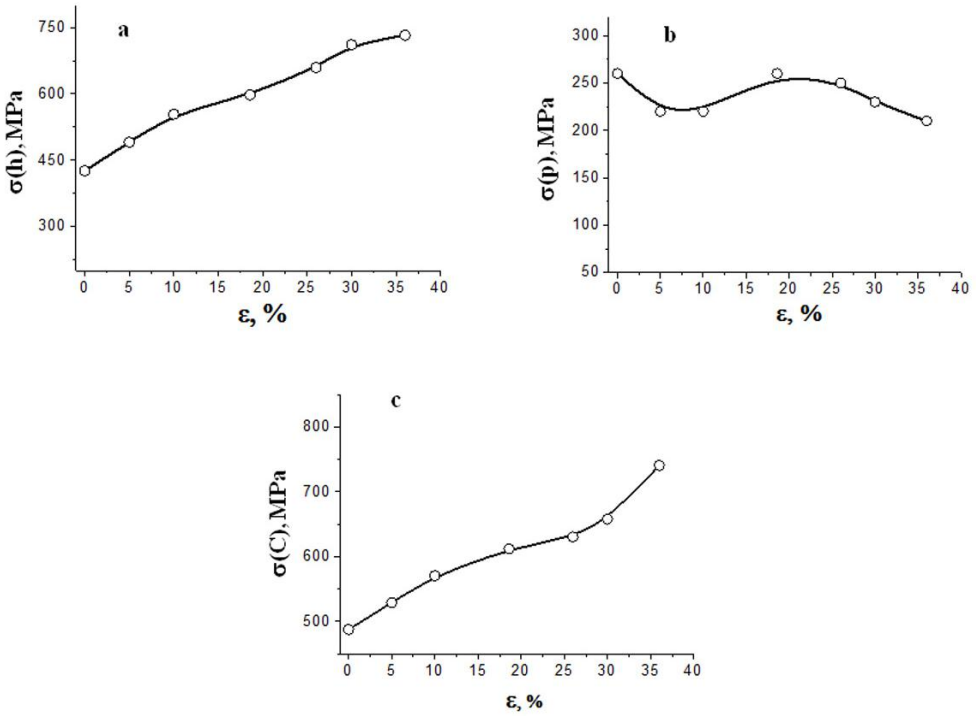

Fig. 12. Dependence of contribution into the flow stress from long-range fields of internal stresses σ(h) (**a**), cementite particles (b) and solid-solution hardening **σ(C)** (c) on deformation degree

Presence of carbon atoms in steel and their penetration into crystal lattice leads to its asymmetric distortion assisting the appreciable hardening of the material.

Hardening of steel in the formation of solid interstitial solutions is usually determined by the main factors: first, disagreement of sizes of atoms of impurity and matrix, second, disagreement of elastic modulus of impurity atoms and matrix. According to Fleischer and Hibbard [41, 42] hardening caused by dimensional and elastic disagreement can be calculated from the relation:

$$\sigma_r = G \cdot \delta_s^{3/2} \cdot \frac{c^n}{m}, \qquad (8)$$

where m =760, $\delta_s = |\delta_G| + \alpha_0 |\delta_a|$ – parameter of disagreement, α_0 = 3 for edge and α_0 =16 for screw dislocations, n = 1/2. In researches [41, 42] it is shown that exponent n can be equal to 1, 1/2, 1/3, 0.3.

The equation (8) is inconvenient for calculating the hardening of solid solution of complex-alloy steels therefore when proposing the additivity of contributions to hardening of separate alloying elements the approximate empirical formula of the following type [10, 29] are used:

$$\sigma_r = \sum_{i=1}^{m} (k_i \cdot c_i), \qquad (9)$$

where k_i – coefficient of hardening of ferrite being the increment of yield point at dissolution of 1 weight % of i element in it, c_i – concentration of i element dissolved in ferrite, weight %. Values of k_i coefficient for different elements are determined experimentally [10, 43, 44].

The decrease in sizes of cementite particles at great degrees of deformation may be indicative of their dissolution and escape of carbon atoms to defects of steel crystal lattice (dislocations, subboundaries and boundaries) and into solid solution based on α-phase.

Carbon enrichment of α-phase of crystal lattice facilitates steel hardening whose value was estimated by the expression (9). The results presented in Fig. 12, c testify that with the increase in degree of steel deformation the value of the given contribution increases varying within 490 to 740 MPa, caused by dissolution of cementite particles, penetration of a part of carbon atoms into iron crystal lattice and precipitation on dislocations.

Comparison of values of contribution to work hardening of hardened steel is shown in Fig. 13. It is clearly seen that the greatest contribution to steel hardening is made by solid solution hardening (curve 2), internal stress fields (curve 3) and substructural hardening (hardening with intraphase boundaries) (curve 1) at the final stage of deforming. A comparatively small hardening is shown by dislocation substructure (curve 4) and particles of carbide phase (curve5).

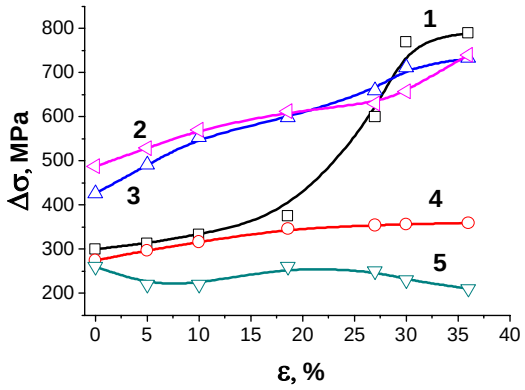

Fig. 13. Dependence of the contribution into the flow stress from intraphase boundaries (1), solid-solution hardening (2), internal stress fields (3), dislocation substructure (4) and cementite particles (5) on deformation degree of steel with a bainite structure

Hence, value of steel work hardening is determined by the availability of a number of mechanisms: friction of matrix lattice, presence of dislocation substructure, particles of carbide phases, intraphase boundaries, carbon atoms and alloying elements dissolved in crystal lattice. It is supposed that total yield point of steel may be represented in terms of linear sum of contribution of separate mechanisms of hardening [10, 44–46]:

$$\sigma = \Delta\sigma_0 + \Delta\sigma(L) + \Delta\sigma(\rho) + \\ + \Delta\sigma(h) + \Delta\sigma(p) + \Delta\sigma(C), \qquad (10)$$

where $\Delta\sigma_0$ – contribution caused by friction of matrix lattice, $\Delta\sigma(L)$ – contribution caused by intraphase boundaries, $\Delta\sigma(\rho)$ – contribution caused by dislocation substructure, $\Delta\sigma(h)$ – contribution caused by long-range fields of stress, $\Delta\sigma(p)$ – contribution caused by the presence of particles of carbide phases, $\Delta\sigma(C)$ – contribution caused by atoms of alloying elements. As seen from the equation (10), principle of additivity suggests the independent action of each of the mechanism of hardening on yield point of the material.

The curves of deformation hardening of steel with bainite structure calculated by the results of estimates of hardening mechanisms (curve 1) and

revealed in the experiment (curve 2) are shown in Fig. 14. It is clearly seen that relation σ-ε obtained in analysis of mechanisms of steel hardening (curve 1) at degrees of deformation increasing ≈15% exceeds the values revealed in experiment (curve 2). With the growth of degree of deformation the disagreement of experimentally obtained and theoretically calculated curves of work hardening increases.

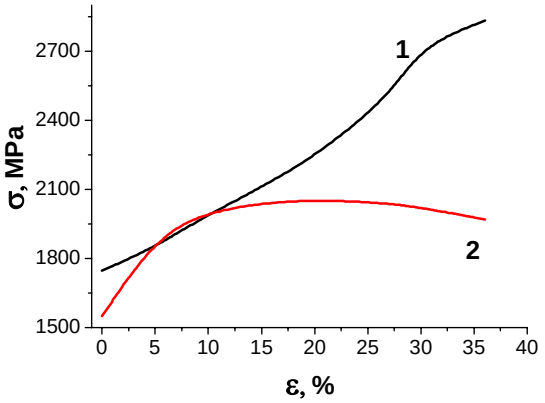

Fig. 14. Curves of steel strain hardening, calculated on the estimation results of the hardening mechanisms (curve 1) and the revealed one during the experiment (curve 2)

Electron microscopy investigations of steel with bainite structure carried out in the research revealed the presence of process of deformation microtwinning. A characteristic image of structure of deformed steel with microtwins is shown in Fig. 8. At degrees of deformation ε = 5% and 10% the deformation twinning of steel is weakly expressed (Fig. 7, b). At greater values of ε the volume fraction of the material covered by deformation microtwinning increases substantially. Hence, on the basis of the results obtained in researches [47, 48] the assumption can be made that the revealed discrepancies of the experimentally obtained and theoretically calculated curves of steel work hardening, that are the most considerable at great degrees of deformation, are caused by the inclusion of microtwinning into the process of steel deformation.

By the present time the fundamental statement has been established that plastic deformation always develops nonuniformly and susceptible to localization not only at microscopic (dislocation) level but at meso- and macrolevels as well [49].

At degrees of deformation 36% and greater the formation of regions of deformation localization placed along interfaces of adjacent plates of bainite or grain boundaries is observed. Their structure is similar to structure of channels observed under drawing deformation of steel 08Mn2Si and compression deformation of hardened steel 38Cr3Ni3MoV [19, 50–52] (Fig. 15, **a**).

Regions of deformation localization in dark field images in matrix reflexes have a tabby contrast. Microelectron diffraction patterns obtained from these regions as a rule have a quasi-ring structure (Fig. 15, b) indicating to the small (50–100 nm) size of crystallites forming them and predominantly wide angular disorientation of crystallites. Channel of deformation has a layer structure resembling the structure of martensite packet. Regions of deformation localization extend to tens of microns in length and reach 0.5 μm in diameter. With growth of degree of deformation the average sizes of deformation channels increase.

Judging from the structure of microelectron diffraction pattern shown in Fig. 15, b the particles of the second phase are present in the volume of deformation channel. Reflexes from the particle of the second phase are highly distorted both in radial and azimuthal directions. This circumstance can be caused by both distortion of crystal lattice of particles and their small sizes [20, 21]. Microelectron diffraction pattern obtained from regions of foil adjacent to the channel are point ones being characteristic of polycrystalline material. With the growth of degree of deformation the volume of material occupied by channels of deformation increases reaching several percents at the moment of steel failure.

In deformation channel the substructure is also fragmented one, however sizes of fragments are far less than in the main volume of the material. In addition, fragments in deformation channel are isotropic in shape. Judged from the size of fragments it should be believed that a shear exceeding several-fold the average one is localized in deformation channel.

The next feature of deformation channel structure is connected with the behavior of extinction contours in them. It should be noted that bend extinction contours mark the regions with the same orientation of concrete planes of reflection relative to falling beam of electrons [20, 21]. It is established that both in deformation channel and in regions adjacent to it the portions of same orientation or close to it and extended approximately parallel to the long side of channel are present. In the context of hydrodynamics the portions such as these are analogous to lines of flow in laminar flow [19, 50–52]. Since under compression a considerable number of portions with turbulent flow come into being as a rule a comparison such as this may throw light on nature of deformation channels. Namely, the conditions of deformation in them are such that work of deformation appears to be lower than in adjacent portions. It may be suggested that local heating of the material plays the main part here [19, 50–52].

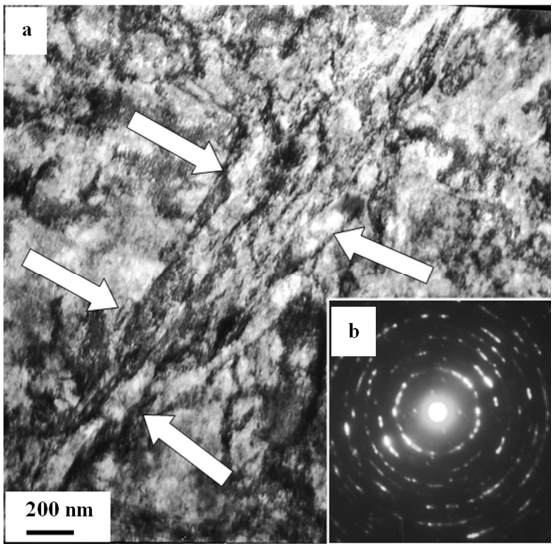

Fig. 15. Channels of deformation being formed in steel 30Cr2Ni2MoV with bainite structure, **ε**=43%; a – light field; b – microelectron diffraction pattern. The channel of deformation is designated with arrows in (a)

One more feature of deformation channels is considerable fields of stress localized inside them and in regions adjacent to them. In [19, 50–52] two mechanisms of relaxation of these stress fields are noted. First, it is done by fragmentation. In this case the chains of fragments of small sizes and close orientation located along the deformation channel are formed. Second, it is done by extension of microcracks. A comparative analysis of structure of deformation channels of bainite steel 30Cr2Ni2MoV and steels 08Mn2Si and 38Cr3Ni3MoV [19, 50–52] is indicative of unified nature of their formation.

4. Conclusion

The investigations of structure, phase composition and defective substructure of steel with bainite structure subjected to plastic deformation were carried out. The quantitative analysis of parameters of steel structure that made it possible to follow the redistribution of carbon atoms in steel structure under plastic deformation was performed. It was established that with growth of degree of deformation the quantity of carbon atoms located in solid solution based on α-iron and defects of crystal lattice as well as cementite particles lying on intraphase boundaries increased; the quantity of carbon atoms forming cementite particles lying in volume of bainite plates and those located in solid solution based on γ-iron decreased.

It was shown that carbide transformations in bainite structure ran in frames of two competitive processes – dissolution of cementite particles having been formed in the process of bainite transformation in volume of ferrite plates, and precipitation of cementite particles on the elements of dislocation substructure in the process of "deformation ageing". Simultaneously with it the additional transformation of retained austenite initiated by steel deforming was observed.

It was shown that plastic deformation by uniaxial compression of steel 30Cr2Ni2MoV with bainite structure is accompanied by: first, increase in scalar density of dislocations and volume of material containing deformation microtwins, second, decrease in average transverse sizes of fragments and increase in degree of their disorientation, third, increase in quantity of stress concentrators and curvature-torsion amplitude of crystal lattice of the material. The stages of changes of steel structure parameters were revealed. The proposal was made about the changing in steel deformation mechanism: at the first stage of loading ($0\% < \varepsilon < 18\%$) deformation was done predominantly by motion of dislocations; at the second stage ($18\% < \varepsilon < 36\%$) – it was done by motion of dislocations and twinning.

It was shown that steel hardening had a multifactor character. The estimates of mechanisms of hardening by boundaries of bainite plates and fragments, scalar density of dislocations, long-range stress fields, cementite particles, and interstitial atoms were carried out. The largest contribution to the value of work hardening of steel under study was made by substructural hardening (hardening caused by long-range internal fields of stresses and fragmentation of structure) and solid solution hardening caused by penetration of carbon atoms into crystal lattice of ferrite.

At degree of deformation $\varepsilon > 36\%$ the formation of channels of localized deformation – particular structural states of material being localized along the interfaces of adjacent plates of bainite or grain boundaries was revealed.

The research was done supported by the grant of the Russian Scientific Fund (project №15-12-00010).

References

1. Ohmori Y., Jung Y.-C., Nakai K., Shiori H. Bainite transformation and the diffusional migration of bainite/austenite broad interfaces in Fe-9%Ni-C alloys // Acta Materialia. 2001. Vol. 49. Iss. 6. P. 3149–3162.
2. Quidort D., Brechet Y.J.M. Isothermal growth kinetics of bainite in 0.5% C steels // Acta Materialia. 2001. Vol. 49. Iss. 20. P. 4161–4170.
3. Sourmail T., Smanio V. Low temperature kinetics of bainite formation in high carbon steels // Acta Materialia. 2013. Vol. 61. Iss. 7. P. 2639–2648.
4. Clarke A.J., Speer J.G., Miller M.K. et al. Carbon partitioning to austenite from martensite or bainite during the quench and partition process: A critical assessment // Acta Materialia. 2008. Vol. 56. Iss. 1. P. 16–22.

5. Borgenstam A., Hillert M., Agren J. Metallographic evidence of carbon diffusion in the growth of bainite // Acta Materialia. 2009. Vol. 57. Iss. 11. P. 3242–3252.
6. Gudremon E. Special steels. Moscow: Metallurgiya, 1966. 1274 p.
7. Matrosov Yu.I., Litvinenko D.A. and Golovanenko S.A. Steel for gas pipelines. Moscow: Metallurgiya, 1989. 288 p.
8. Pavlov V.V., Godik L.A., Korneva L.V., Kozyrev N.A., Kuznetsov E.P. Railway rails from bainite steel // Metallurg. 2007. Iss. 4. P. 51–53.
9. Novikov I.I. Theory of thermal treatment of metals. Moscow: Metallurgiya, 1978. 392 p.
10. Pikering F.B. Physical metallurgy and development of steels. Moscow: Metallurgiya, 1982. 184 p.
11. Kurdjumov V.G., Utevskii L.M. and Entin R.I. Transformations in iron and steel. Moscow: Nauka, 1977. 236 p.
12. Bhadeshia H.K.D.H. Bainite in Steels. 2nd ed. The Institute of Materials London, 2001. 460 p.
13. Lee S.-J., Park J.-S., Lee Y.-K. Effect of austenite grain size on the transformation kinetics of upper and lower bainite in a low-alloy steel // Scripta Materialia. 2008. Vol. 59. Iss. 1. P. 87–90.
14. Sourmal T., Smanio V. Low temperature kinetics of bainite formation in high carbon steels // Acta Materialia. 2013. Vol. 61. Iss. 7. P. 2639–2648.
15. Fucheng X. and Luyut Ch. Bainite steels with ultra-low content of carbon and prospects of their application // Problems of Materials Science. 2008. Vol. 53. Iss. 1. P. 52–61.
16. Fang H.-S., Yang J.-B., Yang Z.-G., Bai B.-Z. The mechanism of bainite transformation in steel // Scripta Materialia. 2012. Vol. 47. Iss. 3. P. 157–162.
17. Speich G. and Swann P.R. Regularities of steel work hardening // J. Iron and Steel Inst. 1965. Vol. 203. Iss. 4. P. 480–485.
18. Belous M.V., Cherepin V.T. and Vasiliev M.A. Transformations on tempering of steel. Moscow: Metallurgiya, 1973. 290 p.
19. Ivanov Yu.F., Kornet E.V., Kozlov Ye.V. and Gromov V.E. Hardened structural steel: structure and mechanisms of hardening. Novokuznetsk: Izd-vo SibGIU, 2010. 174 p.
20. Utevskii L.M. Diffraction electron microscopy in physical metallurgy. Moscow: Metallurgiya, 1973. 584 p.
21. Hirsh P., Khovi A., Nikolson R., Pjeshli D. and Uelan M. Electron microscopy of thin crystals. Moscow: Mir, 1968. 574 p.
22. Pridantsev M. V., Davydova L. N. and Tamarina A. M. Structural Steel Handbook. Moscow: Metallurgiya, 1980. 288 p.
23. Koneva N.A. and Kozlov Ye.V. Nature of substructural hardening // Russian Physics journal. 1982. Iss. 8. P. 3–14.
24. Koneva N.A., Kozlov Ye.V., Trishkina L.I. and Lychagin D.V. The long-range stress fields, curvature-torsion of the crystal lattice and the stage of plastic deformation. Measurement methods and results // Proceedings of the International Conference "New Methods in Physics and Mechanics of Deformed Solid Body". Tomsk: TGU, 1990. P. 83–93.
25. Naulor I.R. The influence of the lath morphology on the yield strength and transition temperature on martensite-bainite steel // Met. Trans. 1979. Vol. 10A. Iss. 7. P. 873–891.
26. Belen'kiy B.Z., Farber B.M. and Goldshtein M.I. Hardness estimates of low-carbon low-alloy steels according to structural data // The Physics of Metals and Metallography. 1975. Vol. 39. Iss. 3. P. 403–409.
27. Trefilov V.I., Moiseev V.I., Pechkovskiy Ye.P. et al. Deformation hardening and failure of polycrystalline metals. Kiev: Naukova dumka, 1987. 248 p.
28. Mac Leen D. Mechanical properties of metals. Moscow: Metallurgiya, 1965. 431 p.
29. Goldshteyn M.I. and Farber B.M. Dispersion hardening of steel. Moscow: Metallurgiya, 1979. 208 p.
30. Shtremel M.A. Strength of alloys. Part II: Deformation. Moscow: MISIS, 1997. 527 p.
31. Predvoditelev A.A. The present state of the art of dislocation ensembles study // Problems of Modern Crystallography. Moscow: Nauka, 1975. P. 262–275.
32. Embyri I.D. Strengthening by dislocations structure // Strengthening Method in Crystals. Applied Science Publishes. 1971. P. 331–402.
33. Static strength and mechanics of failure of steels: Collected articles, translated from German / Edited by V. Dal', V. Anton. Moscow: Metallurgiya, 1986. 566 p.
34. Hall E.O. The deformation and ageing of mild steel: III discussion of results // Proc. Phys. Soc. 1951. Vol. 64B. P. 747–753.
35. Lukke K. and Gottshtejn G. Atomic mechanisms of plasticity of metals // Static strength and mechanics of failure of steels: Collected articles, translated from German / Edited by V. Dal', V. Anton. Moscow: Metallurgiya, 1986. P. 14–36.
36. Dal' V. Increase in strength at the expense of grain refinement // Static strength and mechanics of failure of steels: Collected articles, translated from German / Edited by V. Dal', V. Anton. Moscow: Metallurgiya, 1986. P. 133–146.
37. Gromov V.E., Kozlov Ye.V., Bazaikin V.I., Cellermaer V.Ya. and Ivanov Yu.F. Physics and mechanics of drawing and forging. Moscow: Nedra, 1997. 293 p.
38. Strunin B.N. On distribution of internal stresses at random arrangement of dislocations // Solid State Physics. 1967. Vol. 9. Iss. 3. P. 805–812.
39. Ashby M.F. Physics of Strength and Plasticity. MIT press Cambridge. Mass. 1969. P. 113.
40. Tekin E., Kelly P.M. Tempering of steel precipitation from iron base alloys. Gordon: Breach, 1965. 283 p.
41. Barnard S.J., Smith G.D.W., Saricaya M., Thomas G. Carbon atom distribution in a dual phase steels: on atom probe study // Scripta met. 1981. Vol. 15. Iss. 4. P. 387–392.
42. Fleischer R.L. Dislocation structure in solution hardened alloys // Electron microscopy and strength of crystals. New York; Wiley: Interscience, 1963. P. 973–989.
43. Vohringer O., Macherauch E. Structure und Mechanische eigenschaft von martensite // H.T.M. 1977. Vol. 32. Iss. 4. P. 153–202.
44. Ridley N., Stuart H. and Zwell L. Lattice parameters of Fe-C austenite of room temperature // Trans. Met. Soc. AIME. 1969. Vol. 246. Iss. 8. P. 1834–1836.
45. Norstrom L.A. On the yield strength of quenched low-alloy lath martensite // Scandinavian J. of Met. 1976. Vol. 5. Iss. 4. P. 159–165.
46. Prnka T. Quantitative relationships between parameters of dispersion precipitations and mechanical properties of steels // Physical metallurgy and heat treatment of steel. 1979. Iss. 7. P. 3–8.
47. Koneva N.A., Kiseleva S.F., Popova N.A. and Kozlov Ye.V. Evolution of internal stresses and density of stored energy under deformation austenite steel 110Mg13 // Deformation and failure of materials. 2013. Iss. 9. P. 38–42.
48. Kiseleva S.F., Popova N.A., Koneva N.A. and Kozlov Ye.V. Effect of transformation twins on excessive density of dislocations and internal stresses of deformed fcc crystal lattice of material // Bulletin of the Russian Academy of Sciences. Physics. 2012. Vol. 76. Iss. 13. P. 70–74.
49. Likhachev V.A., Panin V.E., Zasimchuk E.E. et al. Cooperative deformation process and localization of deformation. Kiev: Naukova dumka, 1989. 320 p.
50. Gromov V.E., Panin V.E., Kozlov Ye. V. et al. Channels of deformation in conditions of electrostimulated drawing // Metallphysics. 1991. Vol. 13. Iss. 11. P. 27–34.
51. Gromov V.E., Petrunin V.A. Localization of plastic deformation under conditions of electrostimulated drawing // Physica stalus Solidi (a). 1993. Vol. 139. P. 77–81.
52. Ivanov Yu.F., Gromov V.E., Kozlov Ye. V., Sosnin O.V. Evolution of channels of localized deformation in the process of electrostimulated drawing of low carbon steel // Izvestiya Vuzov. Ferrous metallurgy. 1997. Iss. 6. P. 42–45.

Материал поступил в редакцию 26.01.16.

ИНФОРМАЦИЯ О СТАТЬЕ НА РУССКОМ ЯЗЫКЕ

DOI:10.18503/1995-2732-2016-14-1-87-100

БЕЙНИТНАЯ СТАЛЬ: СТРУКТУРА И ДЕФОРМАЦИОННОЕ УПРОЧНЕНИЕ

Громов В.Е.[1], Никитина Е.Н.[1], Иванов Ю.Ф.[2,3], Аксенова К.В.[1], Семина О.А.[1]

[1] Сибирский Государственный Индустриальный Университет, Новокузнецк, Россия

[2] Институт Сильноточной Электроники Со РАН, Томск, Россия

[3] НИУ Томский Политехнический Университет, Томск, Россия

Аннотация. С использованием методов просвечивающей электронной микроскопии проведен анализ количественной оценки дефектной и карбидной подсистем среднеуглеродистой стали с бейнитной структурой при деформации сжатием до 36%. Проведен количественный анализ перераспределения углерода, а также установлена зависимость концентрации атомов углерода в кристаллической решетке α- и γ-железа, в структурных дефектах, в частицах цементита, расположенных в объеме бейнитных пластин и на межфазных границах, от степени деформации.

Показано, что по мере увеличения степени деформации скалярная плотность дислокаций, объем материала с деформационными двойниками, количество концентраторов напряжений, амплитуда кривизны-кручения кристаллической решетки, степень разориентировки фрагментов увеличиваются, а средние продольные размеры фрагментов уменьшаются. Выполнена оценка дальнодействующих полей напряжений. Обсуждены возможные причины стадийности изменения параметров карбидной фазы и дислокационной субструктуры при деформации.

Проведена оценка механизмов упрочнения с учетом границ пластин и фрагментов, скалярной плотности дислокаций, дальнодействующих полей напряжений, цементитных частиц, атомов внедрения. Показано, что наибольший вклад в деформационное упрочнение исследуемой стали вносит субструктурное упрочнение (упрочнение, обусловленное внутренними дальнодействующими полями напряжений и фрагментацией структуры) и твердорастворное упрочнение вследствие внедрения атомов углерода в кристаллическую решетку феррита.

Сделано предположение, что причиной разупрочнения стали с бейнитной структурой при высокой степени деформации (более 15%) является развитие деформационного микродвойникования.

Ключевые слова: упрочнение, бейнит, деформация, цементит, дислокационная субструктура, механизмы упрочнения, сталь.

Bainite steel: structure and work hardening / Gromov V.E., Nikitina E.N., IvanovYu.F., Aksenova K.V., Semina O.A. // Вестник Магнитогорского государственного технического университета им. Г.И. Носова. 2016. Т. 14. №1. С. 87–100. doi:10.18503/1995-2732-2016-14-1-87-100

Gromov V.E., Nikitina E.N., IvanovYu.F., Aksenova K.V., Semina O.A. Bainite steel: structure and work hardening. *Vestnik Magnitogorskogo Gosudarstvennogo Tekhnicheskogo Universiteta im. G.I. Nosova* [Vestnik of Nosov Magnitogorsk State Technical University]. 2016, vol. 14, no. 1, pp. 87–100. doi:10.18503/1995-2732-2016-14-1-87-100